8. The Michelson Interferometer

8.1 Introduction

Interference patterns from superposed coherent waves may be used for precise determination of wavelength or, if the wavelength is known, time-of-flight, path length or other optical parameters (cf. labs I, Spm and MW). In the present experiment the *Michelson Interferometer* will be used to determine the refractive index of air.

Some safety considerations: The interferometer is a delicate instrument and should be handled with great care. Remove the plastic protection only for adjustment, and put it back in place before any measurements are made. Never expose your eyes to the light of the mercury lamp, neither directly nor through the instrument. Never touch any optical components, in particular not the mirrors.

8.2 Theory

a) The Michelson Interferometer

The design of a Michelson interferometer is schematically outlined in Fig. 8.1. The instrument is designed for investigation of interference between coherent electromagnetic waves from a single monochromatic source. For this purpose, the wave entering the interferometer is split by a semi-transparent mirror (*beam splitter*) into two perpendicular beams and brought to interfere after successive reflections. The physical beam paths, each terminated by reflecting mirrors are sometimes called *interferometer arms*. The *geometrical path length* of an arm may be varied by moving the mirror at its end. The mirror may be mechanically coupled to some external device, thus allowing determination of mechanical translation to a precision of the order of a fraction of a wavelength (for visible light $\sim 10^{-7}$ m). In the experiment performed here, the geometrical path length remains unchanged, but the *optical path length* will be changing with the pressure in a gas cell installed in one arm.[1] A path with geometrical path length d has the optical path length nd, where n is the refractive index of the medium in which the wave travels.

The light source Q is indicated by a light bulb, but the actual source may be of many different kinds. In this laboratory a low-pressure mercury vapour lamp is used, a source that emits light

---

[1]Geometrical path length could be determined with a ruler; optical path length, in principle, by counting the number of wavelengths.
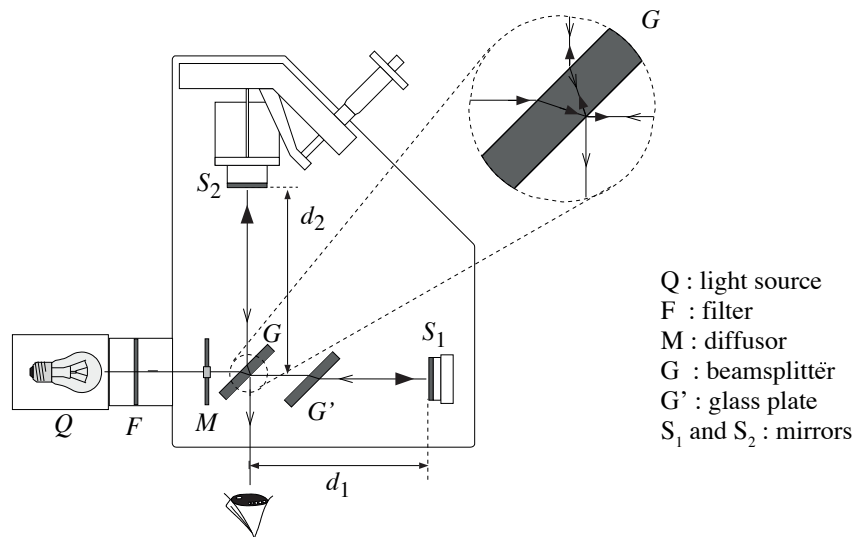
Figure 8.1: Principles of the Michelson interferometer (plane view).

only at discrete, well defined wavelengths. A filter F is employed to suppress light of wavelengths other than the green line of the mercury spectrum. Further requirements on the source that will not be discussed in detail here, is that of *spatial coherence*, meaning that the wave entering the interferometer must retain a constant phase relation (one might think in terms of *wave fronts*) over the cross section of the beam, which in practice may be achieved using an entrance collimator (small hole or slit). The wave must also posses *temporal coherence*, requiring the source to be phase stable for a period of time (the *coherence time*) at least as long as it takes the wave to travel a distance of the order of the *difference* in optical length of the interferometer arms. The coherence time is related to the more familiar notion *coherence length* through the speed of light in the medium. One might think of the source as emitting coherent *wave trains* of the same extension as the coherence length. The mercury lamp emits light with good coherence.

A beam from the light source is incident on the glass plate G, which is coated on the side seen from mirror S_1 with a thin layer of *chromel*.[2] making it a semitransparent mirror, here employed as *beam splitter*. About half of the intensity of the incident light is reflected from the metal layer of plate G in the direction of mirror S_2, then returned and passed through the glass plate G to the observer. The part of the incident light not reflected in G is transmitted through the plate and the metal coating, reflected at mirror S_1 and returned back to G, where it is reflected by the metal layer towards the observer and the two beams interfere.

Between plate G and mirror S_1 the wave travels twice through a second glass plate G', the *compensator*, which to optical precision has the same orientation, the same thickness, and is made of the same quality of glass as used for plate G but without a metal coating. The compensator, as the name suggests, compensates for the difference in optical path length between the two beams of the interferometer that occurs because the beam reflected to mirror S_2 passes three times through the optically denser medium of the glass plate G, whereas the beam transmitted to mirror S_1 passes only once (cf. insert of Figure 8.1 and note that the silver coating on G is facing mirror S_1).

---

[2]An alloy consisting mainly of nickel and a small part of chromium.

With correct compensation for any optical path difference that relates to the design of the instrumental, it suffices to make calculations on the observed changes in the interference pattern to extract information about e.g. a transverse motion of one mirror or a change in refractive index in one of the beams.

Mirror S_2 is mounted on a parallel sliding fixture, cf. Figure 8.1. A micrometer and a spring loaded cantilever is provided for adjustment, so that the mirror can be translated along the direction of the beam, only changing the distance d_2, but not the orientation of the mirror. Distance d_1 to mirror S_1 is fixed, but there is a pair of knurled knobs for tilting horizontally and vertically in order to align the mirror perpendicular to the beam.

The mercury lamp has sufficient spatial coherence to allow a wide window opening. A diffusing screen M is placed after the filter in order to even the light intensity from the lamp. The screen acts as a secondary source that retains the phase relation of the outgoing wave from the source Q.

Interference at the optical axis

At first we restrict the discussion and consider only a point source at the optical axis. As the two waves recombine at the optical axis, their intensities are superimposed (added). It is the relative phase of the two waves that determines the pattern.

If both arms were of identical (optical) length, both waves would arrive with the same phase and interfere constructively (the optical axis corresponds to the centre of the extended interference pattern in Fig. 8.3). This would also be the case if there is a difference in path length of an integer number of wavelengths. We may think of this situation as if wave crests were added from the two waves, which is the condition for constructive interference, resulting in a bright fringe at the centre of the interference pattern.

For the Michelson interferometer there is a slight complication to consider, though. The metal coating on the back of beam splitter G separates an optically denser medium (glass) from a thinner (air). Therefore the beam travelling towards mirror S_2 is in effect reflected inside the glass plate, off an optically thinner medium; the beam returning from mirror S_1 in air is reflected from the metal film applied on the denser medium (glass). In the latter case, for reasons that are not obvious, a phase shift of π occurs, corresponding to a change in the optical path of $\lambda/2$. In the former case there is no change.

For paths of equal optical length, or with a difference of an integer number of wavelengths, the additional $\lambda/2$ difference therefore causes a wave crest of one beam to be added to a trough of the other, such that actually destructive interference occurs, and therefore a dark fringe appear in the centre of the pattern.

Disregarding, for a moment, the additional $\lambda/2$, the general condition for interference may thus be expressed as follows, using ΔW_0 for the path difference at the optical axis ($\theta = 0$), cf. Fig. 8.2.

With λ designating the wavelength and $m = 0, 1, 2 \ldots$ an integer number, constructive interference, i.e. maximum intensity (a bright fringe at the centre) occurs if:
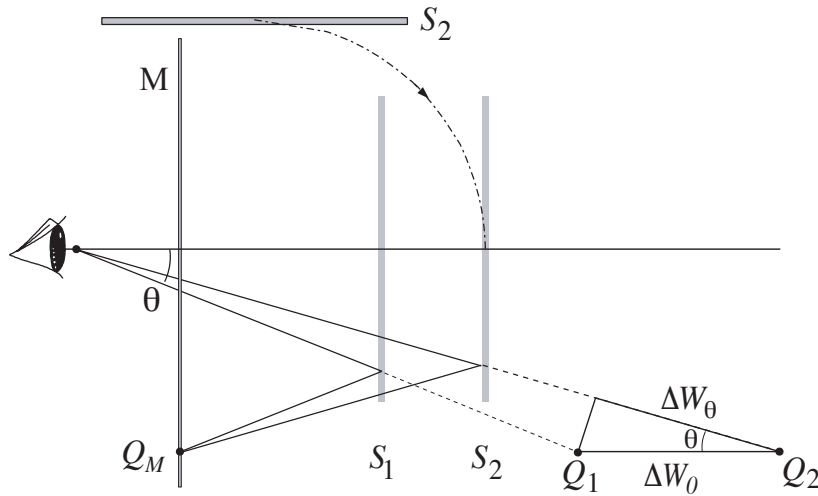
$$\Delta W_0 = m \cdot \lambda \tag{8.1}$$

Figure 8.2: Interference from an off-axis point source Q_M on the diffusing plate M.

In words, this relation tells us that the path difference ΔW_0 corresponds to m full wavelengths. Destructive interference, i.e. minimum intensity, accordingly occurs under the condition:

$$\Delta W_0 \;=\; \frac{2m+1}{2} \cdot \lambda \tag{8.2}$$

Taking the additional phase shift introduced in the beam splitter into account, as is necessary for the special case of the Michelson interferometer, $\lambda/2$ would be added on the left of the formulas above, so that the bright centre fringe would become dark, and vice versa.

The extended interference pattern

In order to understand the origin of the extended interference pattern (Fig. 8.3), we must consider light coming from off-axis points on the extended light source, i.e. plate M. Figure 8.2 shows a *linear beam path equivalent* of the Michelson interferometer, and explains how the interference pattern comes about. In order to facilitate the analysis, the two optical paths of the instrument have been joined in the figure in such way that they appear on the same optical axis, but with the correct distances d_1 and d_2; the beam splitter G has been omitted and only the diffusive plate M is shown with the two mirrors. In effect, the axis containing the observer and mirror S_2 has been rotated through 90°, as indicated, to become aligned with the optical axis of S_1.

In Figure 8.2 light is entering the system of mirrors from an arbitrarily chosen point source Q_M, for generality chosen not to lie on the optical axis. The figure depicts a situation where the optical paths are of unequal length (here $d_1 < d_2$) so that the arbitrary point source Q_M, seen by the observer under angle θ from the optical axis, gives rise to the separate coherent image sources, Q_1 and Q_2 respectively.

Unequal optical paths are necessary for an interference pattern to appear: If the two paths were equal, the mirrors in Fig. 8.2, M_1 and M_2 would coincide, as would the mirrored sources Q_1 and Q_2. There would be interference, but for an optically perfect instrument, the conditions would be

the same on the optical axis as in all directions θ viewed by the observer, resulting in a degenerate pattern that covers the entire field of view with the same intensity (in practice this does rarely occur because of imperfections in the optical components).

All source points on plate M seen under the same angle θ_n radiate with the same phase, the reason being that the actual light source behind the plate M radiates coherently, approximately from a single point. The same interference condition therefore applies on a conical surface with top angle 2θ with the observer at the apex, resulting in a set of circular interference fringes, one for each different m (see Fig. 8.3 where the optical axis of the interferometer goes perpendicularly through the center). Because of imperfections in mirrors and other optical components, the actual pattern may appear to be quite distorted. This is, however, of no great concern for the measurement.
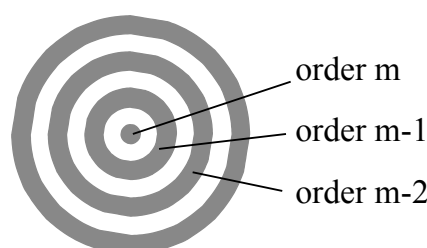

Figure 8.3: Photograph of an interference pattern of concentric circular fringes under perfect conditions.

We now calculate the conditions for interference in different directions θ from the optical axis. Again, we must keep in mind the $\lambda/2$ that enters because of the beam splitter. We write as before ΔW_0 for the path difference at the optical axis ($\theta = 0$), and ΔW_θ for the path difference in the direction θ from the optical axis, see Fig. 8.2.

The interference conditions leading to the the pattern in Fig. 8.3, may be qualitatively understood as follows: On the optical axis interference results in a bright fringe (a centre spot) if the path difference W_0 corresponds to an integer number of wavelengths, m, the additional $\lambda/2$ from the beam splitter being taken into account. The integer m is called the *order of interference*. In some direction θ from the optical axis, where the path difference is W_0 minus one full wavelength, i.e. a total of $m - 1$, the condition is (the path length difference and the diffraction order $(m - n)$ decreases with increasing angle θ):

$$\Delta W_\theta \;=\; (m - 1) \cdot \lambda \tag{8.3}$$

The corresponding angle θ is the direction from the observer where the first bright fringe (a ring) outside the central spot is seen, and we may calculate it as follows. From the triangle in Fig. 8.2 we immediately find that:

$$\Delta W_\theta \;=\; \Delta W_0 \cdot \cos\theta \tag{8.4}$$

Using Eq. 8.1 and Eq. 8.3 for we obtain:

$$\cos\theta \;=\; \frac{(m-1) \cdot \lambda}{m \cdot \lambda} \;=\; \frac{m-1}{m} \tag{8.5}$$

In the direction θ_n the observer sees the $(m-n)$th order of interference ($(m-n)$th fringe in Fig. 8.3). We may calculate this angle using a simple generalisation of the previous argument leading to Eq. 8.5:

$$\cos\theta_n = \frac{(m-n)\cdot\lambda}{m\cdot\lambda} = \frac{m-n}{m} \tag{8.6}$$

By the straightforward geometrical argument used above, we are able to understand why the condition for interference repeats itself for every integer number $m-n$ i.e. the number of full wavelengths accommodated in the path difference, and why the corresponding angle θ increases with n (m kept constant).

Investigating Eq. 8.6, we find that for decreasing path difference ΔW_0 (i.e. decreasing m), the angle θ_n for a particular ring (fixed n) will increase. To the observer operating the interferometer this appears as if the interference fringes (the rings) move outward. Finally, in the limit where the path difference disappears, the pattern of rings collapses into one centre fringe covering the entire field of viewing.

Accordingly for bright fringes, the condition Eq. 8.2 would give us an equivalent expression.

The basic interferometric measurement

We are now ready to perform a simple experiment. The fringe (ring) at a chosen point of reference in the pattern, seen by the observer under angle θ, is assigned the ordinal number 0. This may be the situation depicted in Fig. 8.2. Assume now, that after some change in the optical path N fringes are counted passing our reference point. The corresponding change in optical path is ΔW_θ, and so we arrive at a relation that we might give the name *the interferometer equation*[3]:

$$N \cdot \lambda = \Delta W_\theta \tag{8.7}$$

This is for any measurement the basic relation between the observed change in the pattern: N fringes counted for the corresponding change in optical path difference ΔW_θ.

Next we need to consider what brings about the change ΔW in the optical path length, or in other words: What is actually being measured with the interferometer? We give only two typical examples here.

Geometrical path length: The movable mirror M_2 may be mechanically coupled to some device performing a translation of the order of wavelengths. The change in d_2 makes the the path difference $\Delta W = |d_1 - d_2|$ change, We count the interference rings passing and determine the translation through Eq. 8.7.

Refractive index: This is the object of the present laboratory. As explained below, provision is made for a gas filling in one arm of the interferometer. There is no change in *geometrical* path length difference. A gas filling at a certain pressure and temperature will cause a change in *optical* path length difference ΔW_θ, which is determined using Eq. 8.7. The refractive index may then be calculated as explained below.

---

[3]Not generally accepted terminology

b) Relationship between the refractive index and the pressure of a gas

The speed of propagation (actually the *phase velocity*) of an electromagnetic wave v is related to the frequency of the wave ν and wavelength λ through:

$$v = \lambda \cdot \nu \tag{8.8}$$

The refractive index of n for an electromagnetic wave propagating in a medium is given by

$$n = \frac{c}{v} \tag{8.9}$$

where c is the speed of light in vacuum (a *fundamental physical constant*) and v the speed in the medium. The frequency of a wave will always remain the same. Therefore we conclude:

$$n = \frac{c}{v} = \frac{\lambda_0}{\lambda} \tag{8.10}$$

with λ_0 the wavelength of the electromagnetic wave in vacuum und λ the wavelength in the medium.

A difference in refractive index between the two paths means that the speed of light is different, thus retarding one path and causing a time delay that results in a relative phase difference.[4]

The reduction of the speed of light in a medium compared to that in vacuum is determined in a complicated way by scattering processes involving molecular electrons. It is the interaction of the electric field of the transmitted wave and the electrons of the medium that is of importance, and therefore it is the *number density* of molecules (number divided by volume: SI unit $[m^{-3}]$) that is important, not their absolute number. (If a beam of light passes through a certain length of a medium, the reduced speed is still the same if the length is doubled.)

The refractive index of a gas sensitively depend on the pressure, and therefore we need to develop a relation between pressure and the refractive index.

First we make the simplified assumption that, for a gas, the refractive index, $n = c/v$, increases linearly with the density of molecules from the value (exactly) 1 for vacuum. This is by no means generally true, but for gases of low pressure, and for visible light, it is good enough (this behaviour is termed *normal dispersion*). Using ν_{mol} for the number of molecules in volume V, we may express this relationship as:

$$n - 1 \propto \frac{\nu_{\mathrm{mol}}}{V} \tag{8.11}$$

Then, using the equation of state for an ideal gas:

$$p \cdot V = \nu_{\mathrm{mol}} \cdot R \cdot T \tag{8.12}$$

where p is the absolute pressure, V the volume of the sample, T the absolute temperature, and R the universal gas constant. Using Eq. 8.12 to modify Eq. 8.11 we arrive at an expression relating the index of refraction to the pressure:

$$n - 1 \propto \frac{\nu_{\mathrm{mol}}}{V} = \frac{p}{T} \tag{8.13}$$

---

[4]Actually the original idea of Albert Michelson and Edward Morley was to perform an experiment (1887) that would detect differences in speed in the two paths because of the presumed *ether wind*.

which at constant temperature T may be written:

$$n - 1 \; = \; a \cdot \frac{p}{T} \qquad \text{or} \qquad n \; = \; 1 + \frac{a}{T} \cdot p \tag{8.14}$$

where a is a factor of proportionality. Written in this way, a/T would appear as the slope in a diagram of n plotted against the pressure p. Under the assumptions made, we have found a *linear* relationship between the refractive index and the pressure, valid for constant temperature. The constant of proportionality a will have to be determined to make the relation useful, and this is the object of our experiment.

c) Measuring refractive indices by means of the Michelson interferometer

The principle of a measurement with the interferometer was established above in Eq. 8.7; it describes what our equipment is able to accomplish. The relationship we would like investigate, our theory, is laid down in Eq. 8.14, where the constant a is unknown. Therefore we need to device a method of analysis that connects experiment with theory such that the constant a can be determined. In essence, this is what experimental physicists is commonly confronted with.

In the present experiment, one path of the interferometer remains unchanged for reference, but the other is modified such that it can receive a filling of gas at different pressures. For this purpose a cylindrical cell of precisely known length L is installed, here in the path containing mirror S_2. The cell has glass windows at both ends, and it is necessary to compensate for the optical path the beam travels through these in order to relate unambiguously a change in the observed pattern to a change in refractive index. This is done by putting two identical windows also in the reference path.

The geometrical path length L of the cell is kept constant. Since the optical path through the gas cell is $n \cdot L$, any observed change in the pattern is therefore related to a change of the refractive index n of the gas in the cell (given that the compensations mentioned above have been properly made).

In order to show that the two paths do not have to be equal, we assume that there is an initial geometrical difference d that remains unchanged throughout the experiment. For the path difference at the lowest pressure attained, $p_{\min}$, at which the corresponding refractive index is $n_{\min}$, we write:

$$\Delta W_{\min} \; = \; d + 2\,L \cdot n_{\min} \tag{8.15}$$

and for some arbitrary pressure p:

$$\Delta W \; = \; d + 2\,L \cdot n \tag{8.16}$$

As we change the pressure from $p_{\min}$, to the arbitrary pressure p, whilst keeping the temperature constant at $T_{\exp}$, the corresponding change in optical path length difference will be:

$$\Delta W - \Delta W_{\min} \; = \; ((d + 2\,L \cdot n) - (d + 2\,L \cdot n_{\min})) \; = \; 2\,L \cdot (n - n_{\min}) \tag{8.17}$$

Thus an initial geometrical path difference d, which we prefer to have for reasons explained elsewhere, does not matter. Again the factor of 2 on the right enters because both paths are traversed

twice. In Eq. 8.7 we may remove index θ since it is valid for any directions from the observer. As the pressure changes from $p_{\min}$ to p, the number of fringes N travelling across the point of reference in the pattern is, using Eqs. 8.7 and 8.17:

$$N = \frac{1}{\lambda} \cdot (\Delta W - \Delta W_{\min}) = \frac{2L}{\lambda} \cdot (n - n_{\min}) \tag{8.18}$$

which we rewrite with a simple algebraic manipulation as:

$$N = \frac{2L}{\lambda} \left((n - 1) - (n_{\min} - 1) \right) \tag{8.19}$$

allowing us to utilise the result in Eq. 8.14:

$$N = \frac{2L}{\lambda} \left(\frac{a}{T} p - \frac{a}{T} p_{\min} \right) = \frac{2L}{\lambda} \frac{a}{T} (p - p_{\min}) \tag{8.20}$$

Finally we arrive at the relation:

$$\frac{N\lambda}{2L} = \frac{a}{T_{\exp}} \cdot \Delta p \tag{8.21}$$

where we defined $\Delta p \equiv p - p_{\min}$ for convenience, and explicitly write $T \equiv T_{\exp}$ for clarity. We have here arrived at a linear relation for the two measurable variables, the accumulated number of fringes N and the corresponding pressure difference Δp. This is the general interferometer equation 8.7 applied to the special case of the present experiment. In particular we should note the important property of Eq. 8.21 that the relation may be plotted with the *same slope a/T* as the linear relation $n(p, T)$ in Eq. 8.14 that we are pursuing, cf. Fig. 8.4.
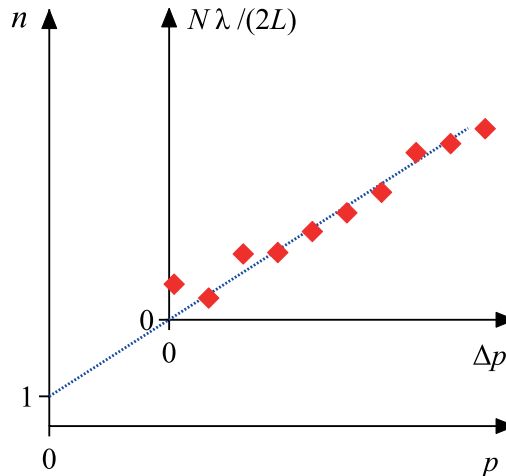

Figure 8.4: Connection between experimental data and theory according to Eqs. 8.21 and 8.14.

In order to simplify the work, we plot only N against the pressure difference Δp, determine the slope b graphically, and calculate the constant of proportionality a:

$$b = \frac{2La}{\lambda T_{\exp}} \qquad \Leftrightarrow \qquad a = b \frac{\lambda T_{\exp}}{2L} \tag{8.22}$$

We have now at hand a complete description of how $n(p, T_{\text{exp}})$ depends on the absolute pressure at constant temperature T_{exp} as formulated by Eq. 8.14.

Note, that the factor of proportionality a cannot be calculated from Eq. 8.21, since the graph produced from the experimental data does not necessarily go through the origin because of unavoidable measurement errors. The slope must be determined graphically as explained below.

Next we acknowledge that the refractive index n is a function of both temperature and pressure, and write in full $n(p, T)$ or $n(p, T_{\text{exp}})$ for a constant temperature T_{exp}.

With the constant of proportionality a experimentally determined, we may write for the pressure dependence of the refractive index (cf. Eq. 8.14):

$$n(p, T_{\text{exp}}) - 1 \;=\; \frac{a}{T_{\text{exp}}} \cdot p \tag{8.23}$$

For comparison with tabulated data, this result may be normalised to the refractive index $n(p_0, T_0)$ at standard conditions p_0 and T_0 (in IUPAC and ISO 2787 p_0=100 kPa and T_0=273.15 K are chosen) using Eq. 8.14 and defining $n(p_0, T_0) \equiv n_0$:

$$n_0 \;=\; 1 + \frac{a \cdot p_0}{T_0} \tag{8.24}$$

In summary, the refractive index of a gas may be calculated at standard conditions for temperature and pressure, if the change in the interference pattern as function of pressure is measured. The wavelength λ of the source, the length L of the gas cell and the constant absolute temperature of the gas T_{exp} are assumed to be known.

8.3 Experimental

Using a Michelson interferometer, in the present experiment the *change* in refractive index of air at constant temperature is calculated from observed changes in the interference pattern as function of pressure. The absolute value of the refractive index at normal conditions is then calculated using information from a set of measurements. A mercury vapour lamp with a wavelength filter is used as light source ($\lambda = 546.1$ nm). The experimental set-up is shown in Fig. **??**. The gas pressure in
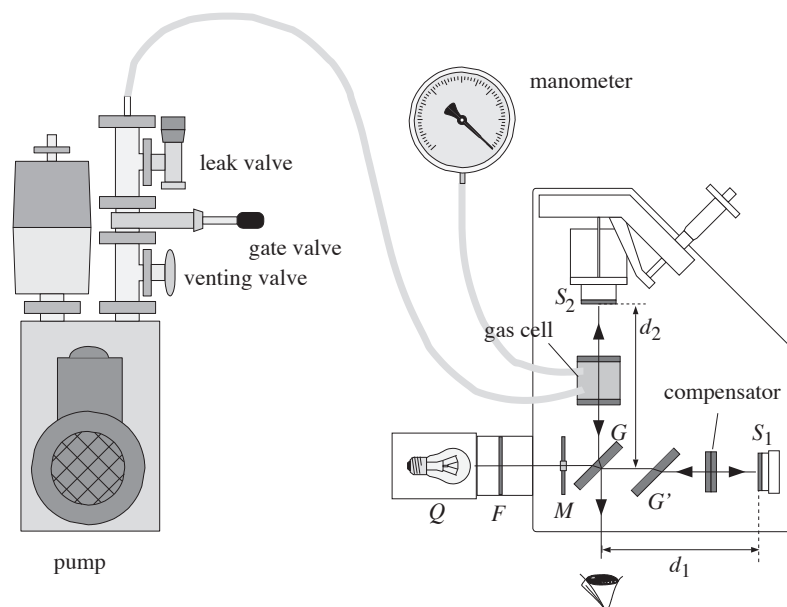
Figure 8.5: Experimental set-up: Side view of pump stand; plane view of interferometer.

the cell may be continuously changed by means of a vacuum pump with a leak valve, and read from a manometer. After adjustments, the interference pattern can be observed through an eyepiece. For ease of adjustment, a pointer Z may be clipped onto the diffusing screen M. Observation is made with an eye aligned with the optical axis of the instrument at a distance of about 25 cm or closer, depending on the eyepiece used. In addition, the tip of the pointer conveniently indicates a point of reference in the pattern that may be used while counting fringes passing as pressure in the gas cell is changed. Adjustment of the interferometer is made as follows:

- Make yourselves acquainted with the apparatus. Make certain that the green filter in place, and switch on the mercury lamp. Carefully remove the plastic protection to gain access to the adjustment knobs. (The protection must be in place during measurement.)

- Write a short hands-on plan for the experiment, later to be included in the experimental part of the report.

- Mirror S_2 is already aligned perpendicular to the beam, and cannot be tilted. Mirror S_1 may be adjusted by means of the two tilt adjustment knobs to position it precisely perpendicular to S_2. If mirror S_1 is far from correct adjustment, two images of the pointer Z should be visible. Using the tilt adjustment knobs the images can be made to coincide horizontally and

vertically. In this position interference fringes should appear. If the adjustment of S_1 is still slightly wrong, almost straight fringes will appear. Turn the tilt adjustment knobs until the centre of the pattern appears in the middle of the viewing field.

- A set of approximately concentric dark and bright ring-shaped interference fringes should now be visible. Use the micrometer on the carrier holding mirror S_2 to change its position. Describe qualitatively how the pattern changes with the distance d_2 Finally choose a setting where the interference fringes are easily distinguished at the tip of Z. Carefully reposition the plastic protection on the instrument.

- Read the temperature T at intervals during the experiment.

- Prepare a table containing columns for the number of fringes counted, accumulated number of fringes N, gauge pressure, absolute pressure p, pressure difference Δp.

- Evacuate the gas cell using the vacuum pump. Then switch off the pump, slowly open the leak valve and observe the interference pattern change as the pressure is increasing. The fringe at the starting pressure (lowest attainable) is given the ordinal number 0. Count the number of fringes as they travel across the tip of the pointer Z and read the pressure p at the manometer for every tenth fringe that pass. Note that *gauge pressure* is indicated (relative to atmospheric pressure), which has to be recalculated to absolute pressure.

- When no further changes can be observed, calculate the difference Δp between each reading and the one with lowest value $p_{\min}$. Draw a diagram and plot N against Δp as shown in Fig. 8.6.
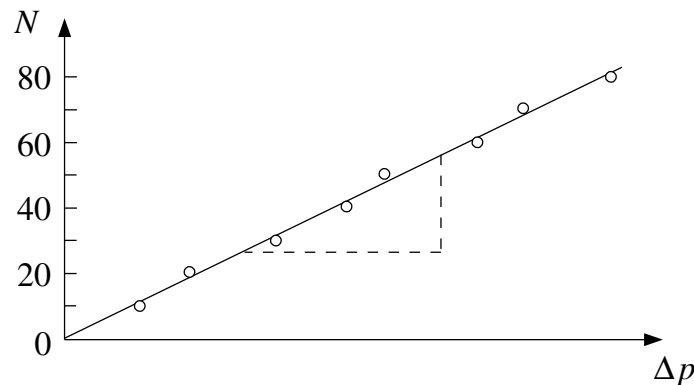

Figure 8.6: Plot of experimental data.

- Repeat the measurement as outlined above, twice for increasing pressure. Plot the results in the same diagram using different symbols for the three data sets. Investigate the diagram to detect any systematic differences between each set of data.

- Estimate by eye, using a ruler, the best linear fit to the data points in the diagram. Note that the origin is not a data point. In the same manner, fit lines representing the steepest and flattest slope that is in accord with the full data set. Determine the slopes b for the three lines, and calculate the factor of proportionality a from Eq. 8.22.

- Calculate the refractive index of air at standard conditions according to Eq. 8.24. Estimate the measurement error from the spread in the slopes of the lines in the diagram. Values for λ and L may be found at the lab bench.